Ray scattering model for spherical transparent particles

Lionel Simonot, Mathieu Hébert, Roger Hersch, Hélène Garay

Ray scattering model for spherical transparent particles

Lionel Simonot,[1,*] Mathieu Hébert,[2] Roger D. Hersch,[2] and Hélène Garay[3]

[1]*PHYMAT (Laboratoire de PHYsique des MATériaux), UMR CNRS 6630, Boulevard Marie et Pierre Curie, BP 179, 86962 Futuroscope Chasseneuil Cedex, France*

[2]*Ecole Polytechnique Fédérale de Lausanne (EPFL), School of Computer and Communication Sciences, Station 14, 1015 Lausanne, Switzerland*

[3]*Ecole des Mines d'Alès, Hélioparc, 2 avenue Pierre Angot, 64053 Pau Cedex 9, France*
**Corresponding author: lionel.simonot@univ-poitiers.fr*

We propose a model for the reflectance of a particle medium made of identical, large, spherical, and absorbing particles in a clear binder. A 3D geometrical description of light scattering is developed by relying on the laws of geometrical optics. The amount of light backscattered by a single particle is determined as a function of its absorbance and refractive index. Then, we consider a set of coplanar particles, called a particle sublayer, whose reflectance and transmittance are functions of the particle backscattering ratio and the particle concentration. The reflectance of an infinite particle medium is derived from a description of multiple reflections and transmissions between many superposed particle sublayers. When the binder has a refractive index different from that of air, the medium's reflectance factor accounts for the multiple reflections occurring beneath the air–binder interface as well as for the measuring geometry. The influences of various parameters, such as the refractive indices and the particle absorption coefficient, are examined.

1. INTRODUCTION

Many opaque objects are composed of a homogeneous medium in which particles of a distinct refractive index are responsible for the scattering of light. The prediction of their color requires establishing the relationship between their reflectance spectrum and the physical properties of their constituting elements. Once every significant parameter of the model has been determined, the spectral reflectance of the objects can be predicted given the conditions of observation and illumination.

The reflectance of a thick particle medium depends on the optical properties of the binder as well as the optical properties, size, shape, relative locations, and concentration of the particles. This high number of relevant parameters gives rise to a large number of models, which are partitioned into the categories of single and multiple scattering models. The first ones focus on the interaction of light with a single particle. They enable the complete description of diffusion in particle media of weak concentration. When the particle concentration is higher, multiple scattering models describe the succession of events undergone by the incident light. They embed parameters representing averaged physical phenomena, e.g., backscattering and absorption, which are either determined by measurement or related to parameters issued from single scattering models.

Mie's theory describes the scattering of waves by a single particle with a simple shape, e.g., a sphere, for any particle size [1,2]. However, as the particle size becomes much larger than the wavelength of light, the incident wave is modeled as a collection of light rays, and Mie's model evolves toward a model of geometrical optics. Scattering involves two types of light rays: Those that hit the particle, which are subject to reflections, refractions, and/or absorption according to the laws of geometrical optics and those that pass very close to the particle and are diffracted [3]. At a large particle size, diffraction becomes insignificant since it represents a small quantity of light, proportional to the particle radius, compared to the quantity of light hitting the particle, proportional to the square of the particle radius.

In most multiple scattering models, the particle medium is assumed to be homogeneous with a random layout of the particles. According to a first approach, qualified as the continuous modelization, an infinitesimal volume element is selected within the homogeneous scattering medium, and the flux variations are described by equations. The radiative transfer equation provides an orientational description of the flux variations for every incoming and outgoing direction [4]. Various methods have been proposed to solve this integrodifferential equation [5,6], but their computation is tedious and time consuming. In the so-called "N-flux models" [7], the flux variations are described for a set of N equal solid angles filling the space by a system of N differential equations. In the case of very densely populated media, only two solid angles are considered, i.e., the upper and the lower hemispheres [8] and a system of two differential equations describes the variations of two opposite diffuse fluxes propagating upward and downward. This continuous two-flux model is known as the Kubelka–Munk model [9,10]. Its differential equation system has analytical solutions giving closed-form expressions for the reflectance and the transmittance of a thick particle layer [10,11].

However, because the flux variations are described at the infinitesimal scale, the continuous models are not directly compatible with a single scattering model, where scattering is described at the noninfinitesimal scale of a particle. As an alternative, multiple scattering can be modeled within a volume element or sublayer having approximately the average size of the particle ("particle volume element" or "particle sublayer"). Corresponding models are qualified as discrete models. A discrete two-flux model describes the multiple scattering in terms of multiple reflections and transmissions between superposed sublayers. Classical formulations have been proposed by Stokes [12], Kubelka [13], and Kortüm [14]. Recent contributions derive an equivalent formulation on the basis of random walks or Markov chains [15–17]. Both the continuous and the discrete two-flux models rely on the same assumption, i.e., a sufficiently high degree of scattering to ensure the uniform angular distribution of the diffuse light.

The first reflectance models for particle media explicitly including a modelization of single scattering by large particles were proposed by Stokes [12] and Bodo [18]. The reflectance of the particle medium was developed according to the discrete two-flux model with the particle sublayer reflectance and transmittance derived from the single scattering model. On the same basis, Melamed [19] in 1963 presented a model for powders and pigments, later refined by Mandelis *et al.* [20] and recently extended by Garay *et al.* [21] to the case of nonspherical particles. Melamed's major contribution concerns the modelization of the particle sublayer reflectance and transmittance. The incident flux, assumed to be diffused after its first penetration into particles, is subject to multiple events of reflection, transmission, and/or absorption inside each particle. The total outgoing flux is calculated and then decomposed into backward, forward, and sideward components. These three components are combined to give the reflectance and the transmittance of a particle sublayer. Due to the sideward component, an attempt is made for modeling lateral scattering within the particle medium. In the calculation of the outgoing flux, the events of reflection, transmission, and absorption are represented by averaged attenuation factors, implicitly assuming that none of these events modifies the Lambertian angular distribution of light. This approximation is suitable for the case of nonideal particles, e.g., with random shapes or rough interfaces, but it fails when particles are spherical and smooth because of the angle-dependence of Fresnel's coefficients and of Beer's attenuation law. During the past decade, Shkuratov and coworkers [22,23] proposed a slightly different model in the domain of astrophysics to interpret the scattering of light by regolithic media on lunar and planetary surfaces. Like Melamed, Shkuratov *et al.* derived the total flux scattered by a single particle from a description of multiple reflections, transmissions, and absorptions of Lambertian light. Afterward the total scattered flux is decomposed into a backward component and a forward component. These two components are calculated according to the following simple model: The rays reflected on the exterior side of the particle are considered as backscattered when they form an acute angle with the incident ray; their contribution to the backward component, given by Fresnel's reflectivity, takes into account the ray orientation. The rays crossing the particle without internal reflection are assumed to be scattered forward, and the rays undergoing internal reflections within the particle are assumed to equally contribute to the forward and backward components. Due to its simplicity, this model does not render well the influence of the particle refractive index and the absorption-dependence of the backward component (see Section 9).

To account for the particle concentration into the particle medium, a "shadowing ratio" is introduced that corresponds to the average probability for the diffuse incident light to strike a particle. Thus, the particle sublayer reflectance and transmittance are combinations of the particle backward and forward components and of this shadowing ratio. The global reflectance of the particle medium is derived from the particle sublayer reflectance and transmittance according to the classical discrete two-flux model.

The model we propose relies on the lines of thought of the model of Shkuratov *et al.*, but with the intent to more rigorously apply the laws of geometrical optics with respect to the ray orientations. We introduce a 3D-vector model giving both the direction and the attenuation of the scattered rays depending on their orientation and their hitting position on the particle. The backward and forward components of the scattered flux are combined together with the shadowing ratio of Shkuratov *et al.* to give the reflectance and the transmittance of a particle sublayer. Then, using the classical discrete two-flux model with the particle sublayer reflectance and transmittance, we determine the reflectance of a semi-infinite particle medium. When the particle medium is observed from a medium different from the binder, e.g., air, we have multiple reflections beneath the air–binder interface. We give the reflectance factor of the interfaced particle medium according to the observation geometry.

This paper is structured as follows. We first recall basic notions of geometrical optics in Section 2. The 3D-vector model is presented in Section 3. It is used to determine the total scattering (Section 4) and the backscattering (Section 5) of diffuse light by a single particle. The reflectance and transmittance of a particle sublayer are presented in Section 6. The discrete two-flux model is used in Section 7 to obtain the reflectance of an infinite particle medium. The reflectance factor accounting for the binder-air interface is given in Section 8. In Section 9, we develop elements of comparison between the model of Shkuratov *et al.* and the present model. Conclusions are drawn in Section 10.

2. LAWS OF GEOMETRICAL OPTICS

A medium is perfectly clear when it is homogeneous, isotropic, nonscattering, and nonabsorbing. It is characterized by its refractive index having a real value. A transparent medium is nonscattering but absorbing. It is characterized by its wavelength-dependent complex refractive index $\hat{n}(\lambda)=n(\lambda)(1+i\kappa(\lambda))$, where $n(\lambda)$ is the real refractive index and $\kappa(\lambda)$ is the attenuation index [[2], p. 219]. The attenuation index characterizes the attenuation of light by the medium, i.e., its absorption. It is related to the linear absorption coefficient $\alpha(\lambda)$ [[2], p. 219]

$$\alpha(\lambda) = \frac{4\pi n(\lambda)\kappa(\lambda)}{\lambda}. \quad (1)$$

According to Beer's law [[2], p. 219], the light traversing a path of length d in a medium with absorption coefficient $\alpha(\lambda)$ is attenuated by the wavelength-dependent factor

$$t(\lambda) = e^{-\alpha(\lambda)d}. \quad (2)$$

A light ray striking a smooth interface between two media i and j, having distinct complex refractive indices $\hat{n}_i$ and $\hat{n}_j$, is reflected and refracted. According to Snell's laws, the incident, reflected, and transmitted light rays belong to a same plane, called the plane of incidence, which also contains the normal of the interface at the point of impact of the incident light ray. The incident angle and the reflection angle are equal. The refraction angle θ_j in medium j is related to the incident angle θ_i in medium i according to

$$n_i \sin\theta_i = n_j \sin\theta_j. \quad (3)$$

The flux fractions being reflected and refracted are given by Fresnel's formulas. They depend on the complex refractive indices of the two media as well as the angle and the polarization of the incident light. In contrast to metals whose attenuation index is high, transparent media have a very low attenuation coefficient. The absorption occurs in the transparent medium volume but not at its interface; the Fresnel coefficients can thus be approximated to depend only on the real refractive indices. Concerning polarization, superscripts s and p denote the electric fields being, respectively, perpendicular and parallel to the incidence plane. The reflectivity of the interface between media i and j, with parallel polarized illumination from medium i at angle θ_i, is

$$R^p_{ij}(\theta_i) = \frac{\tan^2(\theta_i - \theta_j)}{\tan^2(\theta_i + \theta_j)} \quad (4)$$

and its transmittivity is

$$T^p_{ij}(\theta_i) = 1 - R^p_{ij}(\theta_i). \quad (5)$$

The reflectivity for identical illumination with a perpendicular polarization is

$$R^s_{ij}(\theta_i) = \frac{\sin^2(\theta_i - \theta_j)}{\sin^2(\theta_i + \theta_j)} \quad (6)$$

and its transmittivity is

$$T^s_{ij}(\theta_i) = 1 - R^s_{ij}(\theta_i). \quad (7)$$

In the following sections, we consider natural incident light, i.e., incoherent and unpolarized incident light denoted by superscript u. Natural incident light is modeled by two components for parallel and for perpendicular polarization [2]. The two components have equal amplitude and are reflected and/or transmitted, possibly multiple times, independently of each other. The different reflections and transmissions of the parallel and perpendicular components are quantified by the reflectivities and transmittivities given by Eqs. (4) and (5) and by Eqs. (6) and (7), respectively. An observer perceives the average of the two polarization components. For natural light reflected by a single interface, the corresponding reflectivity is

$$R^u_{ij}(\theta_i) = \tfrac{1}{2}(R^s_{ij}(\theta_i) + R^p_{ij}(\theta_i)). \quad (8)$$

To simplify the notation of the following equations, polarization is not specified. Reflectivities and transmittivities are simply noted as $R_{ij}(\theta)$ and $T_{ij}(\theta)$.

When angles θ_j and θ_i are related according to Eq. (3), we have

$$T_{ji}(\theta_j) = T_{ij}(\theta_i) \quad (9)$$

and therefore

$$R_{ji}(\theta_j) = R_{ij}(\theta_i). \quad (10)$$

If $n_j > n_i$, the light rays incident from medium j at an angle θ_j higher than the critical angle $\arcsin(n_i/n_j)$ are totally reflected. Therefore, in that case

$$R_{ji}(\theta_j) = 1,$$

and

$$T_{ji}(\theta_j) = 0. \quad (11)$$

The reflectance of a flat interface illuminated by Lambertian light is called diffuse reflectance. For an illumination from medium i, it is derived from Fresnel's reflectivity according to [24]

$$r_{ij} = \int_{\theta_i=0}^{\pi/2} R_{ij}(\theta_i)\sin 2\theta_i \mathrm{d}\theta_i. \quad (12)$$

Since the energy is conserved at the interface, $1-r_{ij}$ corresponds to the diffuse transmittance of the interface for an illumination from medium i

$$t_{ij} = 1 - r_{ij}. \quad (13)$$

When the interface is illuminated from medium j, its diffuse reflectance and transmittance are noted as r_{ji} and t_{ji}, respectively. Transmittances t_{ij} and t_{ji} are related according to [25]

$$t_{ji} = (n_i/n_j)^2 t_{ij}. \quad (14)$$

From Eqs. (13) and (14), we obtain the relation between the diffuse reflectances r_{ji} and r_{ij}

$$1 - r_{ji} = (n_i/n_j)^2(1 - r_{ij}). \quad (15)$$

3. DIFFUSE ILLUMINATION OF A SPHERICAL PARTICLE

A spherical particle illuminated with Lambertian light receives a collection of light rays that are reflected and refracted at the particle surface. The direction and the proportion of reflection and refraction for each incident ray depend on their orientation in space and striking position on the particle. To precisely specify the orientation and the striking position of rays, we introduce a 3D-vector model. This model combined with the rules of radiometry gives the flux received by the particle as well as the flux reflected at its surface.

A. Three-Dimensional-Vector Model

The Lambertian incident light comes from the upper hemisphere. It is composed of light rays whose direction is

specified by a unit vector **L** oriented "upward," i.e., within the upper hemisphere. The propagation direction is specified by the opposite unit vector $-\mathbf{L}$. In the classical Cartesian coordinates system (x,y,z), the coordinates of vector **L** are

$$\mathbf{L}=\begin{pmatrix}\sin\psi\cos\phi\\ \sin\psi\sin\phi\\ \cos\psi\end{pmatrix}$$

with $0\le\psi\le\pi/2$ and $0\le\phi\le2\pi$ (Fig. 1). However, due to the azimuthal isotropy of spheres, we may only consider light rays whose direction **L** belongs to the xz plane $(\phi=0)$

$$\mathbf{L}=\begin{pmatrix}\sin\psi\\ 0\\ \cos\psi\end{pmatrix}. \tag{16}$$

Light rays oriented according to vector **L** illuminate a half-sphere inclined according to vector **L** (Fig. 1). The point where a given **L** directed ray hits the particle is specified by a unit vector **G** characterized by angles (θ_1,ϕ_1) in respect to **L**. Since **G** coincides with the normal of the particle surface at the illumination point, angle θ_1 formed by **G** and **L** is the ray's local incident angle $(0\le\theta_1\le\pi/2)$. Angle ϕ_1 is the angle between **G** and the xz plane $(0\le\phi_1\le2\pi)$. We consider a new orthogonal coordinate system (x',y',z'), where the z'axis corresponds to vector **L** and the y' axis is identical to the y axis. In this coordinate system, vector **G** has the coordinates

$$\mathbf{G}'=\begin{pmatrix}\sin\theta_1\cos\phi_1\\ \sin\theta_1\sin\phi_1\\ \cos\theta_1\end{pmatrix}, \tag{17}$$

and vector **L** has the coordinates

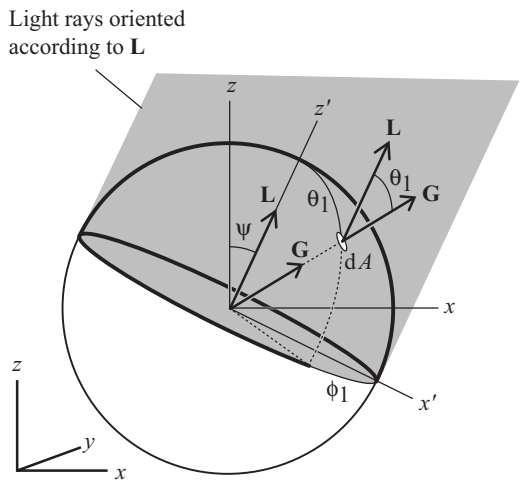

Fig. 1. Light ray coming from direction **L** hitting a surface element dA located according to vector **G**. The bold half-sphere represents the area illuminated by the **L** directed light rays.

$$\mathbf{L}'=\begin{pmatrix}0\\ 0\\ 1\end{pmatrix}. \tag{18}$$

To obtain the classical (x,y,z) coordinates of **G**, we apply to the (x',y',z') coordinates a rotation of angle $-\psi$ around the y axis

$$\mathbf{G}=\begin{pmatrix}\cos\psi & 0 & \sin\psi\\ 0 & 1 & 0\\ -\sin\psi & 0 & \cos\psi\end{pmatrix}\begin{pmatrix}\sin\theta_1\cos\phi_1\\ \sin\theta_1\sin\phi_1\\ \cos\theta_1\end{pmatrix}$$
$$=\begin{pmatrix}\cos\psi\sin\theta_1\cos\phi_1+\sin\psi\cos\theta_1\\ \sin\theta_1\sin\phi_1\\ \cos\psi\cos\theta_1-\sin\psi\sin\theta_1\cos\phi_1\end{pmatrix}, \tag{19}$$

where the 3×3 matrix characterizes the rotation [26]. As expected, the dot product $\mathbf{L}\cdot\mathbf{G}$ gives the cosine of the local incident angle θ_1.

B. Diffuse Incident Flux

Let us consider a Lambertian light source of irradiance E_i. We calculate the corresponding flux Φ_i received by the particle. Every light ray striking the particle corresponds to a same radiance $L_i=E_i/\pi$ and therefore to a flux element [27]

$$\mathrm{d}^2\Phi_i(\mathbf{L},\mathbf{G})=\frac{E_i}{\pi}\mathrm{d}A\cos\theta_1\mathrm{d}\omega, \tag{20}$$

where $\mathrm{d}A=r^2\sin\theta_1\mathrm{d}\theta_1\mathrm{d}\phi_1$ is the elementary surface illuminated by the light ray, r is the particle radius, and $\mathrm{d}\omega=\sin\psi\mathrm{d}\psi\mathrm{d}\phi$ is the infinitesimal solid angle containing radiance L_i. Therefore,

$$\mathrm{d}^2\Phi_i(\mathbf{L},\mathbf{G})=\frac{E_i}{\pi}r^2\cos\theta_1\sin\theta_1\mathrm{d}\theta_1\mathrm{d}\phi_1\sin\psi\mathrm{d}\psi\mathrm{d}\phi. \tag{21}$$

The set of **L** directed light rays illuminating the particle forms a flux element $\mathrm{d}\Phi_i(\mathbf{L})$. It is the sum of all flux elements $\mathrm{d}^2\Phi_i(\mathbf{L},\mathbf{G})$ for $0\le\theta_1\le\pi/2$ and $0\le\phi_1\le2\pi$. Then, summing up the flux elements $\mathrm{d}\Phi_i(\mathbf{L})$ over the upper hemisphere, i.e., for $0\le\psi\le\pi/2$ and $0\le\phi\le2\pi$, we obtain the total flux Φ_i received by the particle

$$\Phi_i=r^2\frac{E_i}{\pi}\int_{\phi=0}^{2\pi}\int_{\psi=0}^{\pi/2}\left[\int_{\phi_1=0}^{2\pi}\int_{\theta_1=0}^{\pi/2}\cos\theta_1\sin\theta_1\mathrm{d}\theta_1\mathrm{d}\phi_1\right]$$
$$\times\sin\psi\mathrm{d}\psi\mathrm{d}\phi=2\pi r^2E_i. \tag{22}$$

C. External Reflectance

Let us now calculate the fraction of Lambertian incident light that is reflected by the particle having a refractive index n_2 and being surrounded by a medium of refractive index n_1. According to Fresnel's formulas, a fraction $R_{12}(\theta_1)$ of each incident flux element $\mathrm{d}^2\Phi_i(\mathbf{L},\mathbf{G})$ is subject to reflection. Therefore, the total flux Φ_r reflected by the particle is

$$\Phi_r = r^2 \frac{E_i}{\pi} \int_{\phi=0}^{2\pi} \int_{\psi=0}^{\pi/2} \left[\int_{\phi_1=0}^{2\pi} \int_{\theta_1=0}^{\pi/2} R_{12}(\theta_1) \times \cos\theta_1 \sin\theta_1 \mathrm{d}\theta_1 \mathrm{d}\phi_1 \right] \sin\psi \mathrm{d}\psi \mathrm{d}\phi. \quad (23)$$

After simplification of Eq. (23), the reflected flux becomes

$$\Phi_r = 2\pi r^2 E_i \int_{\theta_1=0}^{\pi/2} R_{12}(\theta_1) \sin 2\theta_1 \mathrm{d}\theta_1. \quad (24)$$

The ratio Φ_r/Φ_i corresponds to the diffuse external reflectance of the particle r_{12} that is identical to the diffuse reflectance of a flat interface given in Eq. (12)

$$r_{12} = \int_{\theta_1=0}^{\pi/2} R_{12}(\theta_1) \sin 2\theta_1 \mathrm{d}\theta_1. \quad (25)$$

The same expression for the reflectance of a spherical interface was derived by Bohren and Huffman [28].

4. SCATTERING OF LIGHT BY A SINGLE PARTICLE

According to the ray-optics model, the scattering of light by a transparent particle is described in terms of ray multiple reflections and transmissions. Reflections occur at the exterior and interior sides of the particle interface. Transmissions occur through the particle interface and through the particle medium with attenuation due to absorption. Let us first consider the case of directional incident light and then the case of Lambertian incident light.

A. Directional Nonabsorbance

A spherical particle of diameter d is surrounded by a clear medium 1 of refractive index n_1. It is made of a transparent medium 2 whose wavelength-dependent refractive index is $n_2(\lambda) > n_1(\lambda)$ and whose wavelength-dependent absorption coefficient is $\alpha(\lambda)$. When a light ray strikes the particle surface, it is reflected and refracted according to Snell's laws. The incident ray, the reflected ray, and the refracted ray as well as the particle surface normal all belong to the plane of incidence. Since the particle is a sphere, the surface normal passes through the particle center whatever the incident angle, and the plane of incidence is an equatorial plane of the particle.

Let us call θ_1 the local incident angle of the ray on the exterior surface of the particle. The reflection angle is equal to θ_1. The refraction angle inside the particle, θ_2, is deduced from Eq. (3). The refracted light ray is subject to multiple reflections within the particle, all occurring in the plane of incidence with a same angle θ_2 (Fig. 2). Between two internal reflections, the ray travels a distance $d \cos\theta_2$ and is attenuated by a factor t according to Beer's law [Eq. (2)]. This attenuation factor may be expressed as a function of θ_1 according to Eq. (3)

$$t(\theta_1) = e^{-\alpha d \cos\theta_2} = e^{-\alpha d \sqrt{1-(n_1 \sin\theta_1/n_2)^2}}. \quad (26)$$

The directional nonabsorbance of the particle, F_S, is the fraction of the incident element of flux that exits the particle without being absorbed. It is the sum of the different exiting components featured in Fig. 2 expressed as the following geometric series:

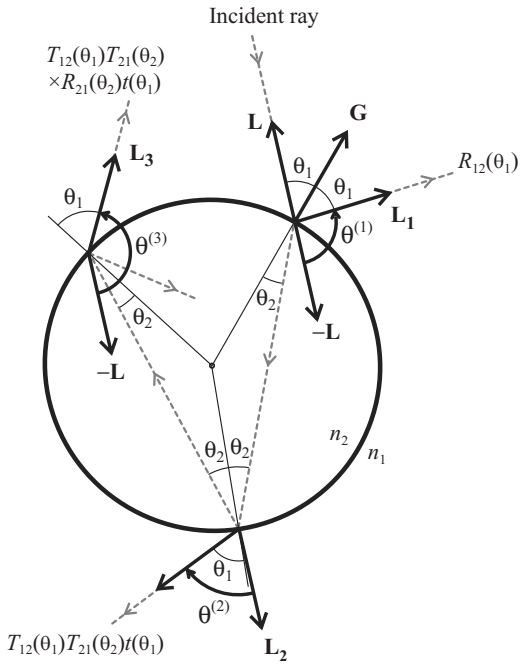

Fig. 2. Multiple reflection of light within a spherical transparent particle of refractive index n_2 surrounded by a medium of refractive index $n_1 < n_2$. All light rays belong to a same plane through the center of the particle.

$$F_S(\theta_1) = R_{12}(\theta_1) + T_{12}(\theta_1)T_{21}(\theta_2)t(\theta_1) \sum_{k=0}^{\infty} [R_{21}(\theta_2)t(\theta_1)]^k. \quad (27)$$

Reducing the geometric series and using Eqs. (5) or (7) and Eq. (9), the directional nonabsorbance of the spherical particle becomes

$$F_S(\theta_1) = R_{12}(\theta_1) + \frac{(1-R_{12}(\theta_1))^2 t(\theta_1)}{1-R_{12}(\theta_1)t(\theta_1)}. \quad (28)$$

B. Diffuse Nonabsorbance

The diffuse nonabsorbance corresponds to the fraction of Lambertian incident flux Φ_i that is scattered, i.e., not absorbed, by the particle. The total flux Φ_i received by the particle is given by Eq. (22). Let us again use the 3D-vector model developed in Section 3 to calculate the scattered flux Φ_S. Every incident light ray is specified by a vector $\mathbf{L}$ for its direction and by a vector $\mathbf{G}$ for its hitting position on the particle. It corresponds to a flux element $\mathrm{d}^2\Phi_i(\mathbf{L},\mathbf{G})$ given by Eq. (20). A fraction $F_S(\theta_1)$ given by Eq. (28) is scattered, where θ_1 is the angle of incidence, formed by $\mathbf{L}$ and $\mathbf{G}$. The corresponding scattered flux is

$$\mathrm{d}^2\Phi_S(\mathbf{L},\mathbf{G}) = F_S(\theta_1)\mathrm{d}^2\Phi_i(\mathbf{L},\mathbf{G}). \quad (29)$$

Following the same reasoning line as in Section 2 from Eqs. (20)–(22), the total scattered flux Φ_S is

$$\Phi_S = r^2 \frac{E_i}{\pi} \int_{\phi=0}^{2\pi} \int_{\psi=0}^{\pi/2} \int_{\phi_1=0}^{2\pi} \int_{\theta_1=0}^{\pi/2} F_S(\theta_1) \cos\theta_1 \sin\theta_1 \times \sin\psi \mathrm{d}\theta_1 \mathrm{d}\phi_1 \mathrm{d}\psi \mathrm{d}\phi = 2\pi r^2 E_i \int_{\theta_1=0}^{\pi/2} F_S(\theta_1) \sin 2\theta_1 \mathrm{d}\theta_1. \quad (30)$$

The particle diffuse nonabsorbance f_S is given by the ratio of scattered flux Φ_S to incident flux Φ_i

$$f_S = \int_{\theta_1=0}^{\pi/2} F_S(\theta_1) \sin 2\theta_1 \mathrm{d}\theta_1, \quad (31)$$

which becomes, according to the expanded expression (28) of directional reflectance and the defining equation (25) of r_{12}

$$f_S = r_{12} + \int_{\theta_1=0}^{\pi/2} \frac{(1 - R_{12}(\theta_1))^2 t(\theta_1)}{1 - R_{12}(\theta_1) t(\theta_1)} \sin 2\theta_1 \mathrm{d}\theta_1. \quad (32)$$

The term $(1-f_S)$ corresponds to the particle's diffuse absorbance. Its expression derived from Eq. (31) is equivalent to the one derived by Mayer and Madronich [29] for water droplets. In the case of perfectly clear particles ($\alpha=0$) there is no absorption, and all the incident light is scattered, i.e., $t(\theta_1)=1$ and $f_S=1$.

5. BACKSCATTERING BY A SINGLE PARTICLE

The reflection of light by a thick particle medium is due to a combination of single scattering by each particle and of multiple scattering between neighboring particles. As a first step for describing multiple scattering, we introduce an extension of the model presented in Section 4, where only the light rays propagated into the upper hemisphere are accounted for. The corresponding fraction of incident light is called the backward component, noted as r_S. It may be expressed as a function of the particle nonabsorbance f_s

$$r_S = x f_S, \quad (33)$$

where x is called the backscattering ratio. The forward component t_S corresponds to the fraction of light scattered forward

$$t_S = f_S - r_S = (1 - x) f_S. \quad (34)$$

A. Backscattered Light Rays

Let us consider an incident light ray characterized by its direction vector $\mathbf{L}$ and its position vector $\mathbf{G}$. We call $\mathbf{L}_N$ the exit direction of the Nth scattered rays, with $N=1,2,3,\ldots$. The angle from $-\mathbf{L}$ to $\mathbf{L}_N$ is called $\theta^{(N)}$. We can deduce from Fig. 2 that

$$\theta^{(1)} = \pi - 2\theta_1, \quad (35)$$

and the recursive formula

$$\theta^{(N)} - \theta^{(N-1)} = 2\theta_2 - \pi, \quad N \geq 1, \quad (36)$$

where $\theta_2 = \arcsin(n_1 \sin\theta_1 / n_2)$ is the refraction angle of the light ray into the particle. We finally obtain the general expression for $N \geq 1$ [2,30]

$$\theta^{(N)} = 2(N-1)\theta_2 - 2\theta_1 - (N-2)\pi \mod(2\pi). \quad (37)$$

Vectors $\mathbf{L}$, $-\mathbf{L}$, $\mathbf{G}$, and $\mathbf{L}_N$ ($N \geq 1$) all belong to the plane of incidence. For every $N \geq 1$, $\mathbf{L}_N$ is the vector issued from $-\mathbf{L}$ by a rotation of angle $\theta^{(N)}$ in the incidence plane. The rotation is carried out counterclockwise for positive angles around the incidence plane normal specified by the unit vector

$$\mathbf{I} = \frac{\mathbf{G} \times \mathbf{L}}{\|\mathbf{G} \times \mathbf{L}\|} = \begin{pmatrix} \cos\psi \sin\phi_1 \\ -\cos\phi_1 \\ -\sin\psi \sin\phi_1 \end{pmatrix}.$$

The rotation according to axis $\mathbf{I}$ and of angle $\theta^{(N)}$ applied to vector $-\mathbf{L}$ is given by the vector rotation formula [26]

$$\mathbf{L}_N = \cos\theta^{(N)}(-\mathbf{L}) + \sin\theta^{(N)} \mathbf{I} \times (-\mathbf{L}), \quad N \geq 1,$$

which yields the following Cartesian coordinates for the vectors $\mathbf{L}_N$:

$$\mathbf{L}_N = \begin{pmatrix} -\cos\theta^{(N)} \sin\psi + \sin\theta^{(N)} \cos\psi \cos\phi_1 \\ \sin\theta^{(N)} \sin\phi_1 \\ -\cos\theta^{(N)} \cos\psi - \sin\theta^{(N)} \sin\psi \cos\phi_1 \end{pmatrix}, \quad N \geq 1.$$

The third component of $\mathbf{L}_N$ corresponds to the cosine of angle $\psi^{(N)}$, formed by the Nth scattered ray in respect to the vertical direction

$$\cos\psi^{(N)} = -(\cos\theta^{(N)} \cos\psi + \sin\theta^{(N)} \sin\psi \cos\phi_1), \quad N \geq 1. \quad (38)$$

The backscattered flux is formed by the scattered rays whose vector $\mathbf{L}_N$ is directed into the upper hemisphere, i.e., $\cos\psi^{(N)} > 0$. To select among all the scattered rays those that are scattered into the upper hemisphere, we introduce the following function:

$$H(\cos\psi^{(N)}) = \begin{cases} 1 & \text{if } \cos\psi^{(N)} > 0 \\ 0 & \text{otherwise} \end{cases}. \quad (39)$$

B. Nth Backscattered Flux

Every incident light ray corresponds to a light flux $\mathrm{d}^2\Phi_i(\mathbf{L},\mathbf{G})$ expressed by Eq. (20). Due to the multiple reflections occurring within the particle, it is decomposed into an infinity of scattered flux components $\mathrm{d}^2\Phi_N(\mathbf{L},\mathbf{G})$, ($N=1,2,3\ldots$), each one being a fraction $F_N(\theta_1)$ of the incident flux element $\mathrm{d}^2\Phi_i(\mathbf{L},\mathbf{G})$. For $N=1$, $F_1(\theta_1)$ corresponds to the Fresnel reflectivity of the exterior particle surface

$$F_1(\theta_1) = R_{12}(\theta_1). \quad (40)$$

For $N \geq 2$, the path followed by the Nth scattered ray includes a refraction into the particle with a Fresnel transmittivity $T_{12}(\theta_1)$, $(N-1)$ travels within the particle with attenuation $t(\theta_1)$, $(N-2)$ internal reflections with Fresnel transmittivity $R_{21}(\theta_2)=R_{12}(\theta_1)$, and a refraction out of the

particle with Fresnel transmittivity $T_{21}(\theta_2)=T_{12}(\theta_1)$. The total attenuation is therefore

$$F_N(\theta_1) = T_{12}^2(\theta_1)R_{12}^{N-2}(\theta_1)t^{N-1}(\theta_1). \tag{41}$$

We call the Nth backscattered flux, Φ_N, the sum of the Nth scattered flux elements directed into the upper hemisphere for all $\mathbf{L}$ and $\mathbf{G}$. Let us sum up the flux elements $H(\cos\psi^{(N)})\mathrm{d}^2\Phi_N(\mathbf{L},\mathbf{G})$ in the same manner as in Section 2 for Eqs. (20)–(22). Due to the azimuthal isotropy of the system, the integrated term does not depend on the azimuthal angle ϕ, and the integral according to angle ϕ yields a factor 2π. We obtain

$$\Phi_N = r^2E_i\int_{\psi=0}^{\pi/2}\int_{\phi_1=0}^{2\pi}\int_{\theta_1=0}^{\pi/2} H(\cos\psi^{(N)})F_N(\theta_1)\sin 2\theta_1 \times\sin\psi\mathrm{d}\theta_1\mathrm{d}\phi_1\mathrm{d}\psi. \tag{42}$$

C. Backward Component

The ratio of the Nth backscattered flux Φ_N given by Eq. (42) to the incident flux Φ_i given by Eq. (22) is called r_N

$$r_N = \Phi_N/\Phi_i, \tag{43}$$

and the backward component r_S is the sum of the r_N

$$r_S = \sum_{N=1}^{\infty} r_N. \tag{44}$$

Since the contribution of the fourth and following scattered rays is low compared to the one of the three first scattered rays, we may simplify r_S by grouping the fourth and following rays into a single term r_{4+}. Equation (44) becomes

$$r_S = r_1 + r_2 + r_3 + r_{4+}. \tag{45}$$

Furthermore, we consider that the fourth and following scattered rays equally contribute on average to the backscattered and forward fluxes. Thus, the backscattered flux is half the total scattered flux Φ_{4+}. Flux Φ_{4+} is derived from a geometric series similar to Eq. (27) with omissions of the first scattered ray (specular reflection), the second scattered ray (exponent $k=0$ in the infinite sum), and the third scattered ray (exponent $k=1$ in the infinite sum) by an angular integration similar to Eq. (30)

$$\Phi_{4+} = r^2\frac{E_i}{\pi}\int_{\phi=0}^{2\pi}\int_{\psi=0}^{\pi/2}\left[\int_{\phi_1=0}^{2\pi}\int_{\theta_1=0}^{\pi/2}(T_{12}(\theta_1)T_{21}(\theta_2)t(\theta_1) \times\sum_{k=2}^{\infty}[R_{21}(\theta_2)t(\theta_1)]^k)\cos\theta_1\sin\theta_1\mathrm{d}\theta_1\mathrm{d}\phi_1\right]\sin\psi\mathrm{d}\psi\mathrm{d}\phi. \tag{46}$$

The reduction of the geometrical series and of the integrals yields

$$\Phi_{4+} = 2\pi r^2E_i\int_{\theta_1=0}^{\pi/2}\frac{T_{12}^2(\theta_1)R_{12}^2(\theta_1)t^3(\theta_1)}{1-R_{12}(\theta_1)t(\theta_1)}\sin 2\theta_1\mathrm{d}\theta_1. \tag{47}$$

Then, the term r_{4+} is given by

$$r_{4+} = \frac{1}{2}\frac{\Phi_{4+}}{\Phi_i} = \frac{1}{2}\int_{\theta_1=0}^{\pi/2}\frac{T_{12}^2(\theta_1)R_{12}^2(\theta_1)t^3(\theta_1)}{1-R_{12}(\theta_1)t(\theta_1)}\sin 2\theta_1\mathrm{d}\theta_1. \tag{48}$$

D. Numerical Evaluations

Figure 3 shows the evolution of the terms r_1, r_2, r_3, r_{4+}, and backward component r_S as functions of the diametrical absorbance αd of the particle for a relative refractive index $n_2/n_1=1.5$. The term r_1 represents the external reflection on the particle and is independent of the particle absorbance. Its expression is given by inserting Eq. (40) into Eqs. (42) and (43)

$$r_1 = \frac{1}{2\pi}\int_{\psi=0}^{\pi/2}\int_{\phi_1=0}^{2\pi}\int_{\theta_1=0}^{\pi/2} H(\cos\psi^{(1)})R_{12}(\theta_1)\sin 2\theta_1 \times\sin\psi\mathrm{d}\theta_1\mathrm{d}\phi_1\mathrm{d}\psi \tag{49}$$

with $\psi^{(1)}=\cos(2\theta_1)\cos\psi-\sin(2\theta_1)\sin\psi\cos\phi_1$ obtained from Eqs. (37) and (38).

Terms r_2, r_3, r_{4+}, and thereby r_S decrease as the particle absorbance increases. For highly absorbing particles, since light is almost completely absorbed during its first travel within the particle, terms r_2, r_3, and r_{4+} are close to zero, and r_S is close to r_1. As expected, the contribution of the fourth and following scattered rays, r_{4+}, is very low compared to the contribution of the first three scattered rays, but it is important to include it in the calculation of r_S to ensure the conservation of energy. Omitting the fourth and following ray contribution r_{4+} represents in the case of multiple scattering a loss of energy comparable to absorption. Even though for a single particle the induced error is small, it is exponentially increased when modeling multiple scattering between several particles.

The backward component, r_S, the particle nonabsorbance, f_S, and the backscattering ratio, x, are plotted in Fig. 4 as functions of the particle's diametrical absorbance αd for a relative refractive index $n_2/n_1=1.5$. In the case of a highly absorbing particle, only the reflection outside the particle yields relevant scattering, and f_S and r_S become independent of the particle absorbance. The backscattering ratio x slightly increases with the particle absorbance.

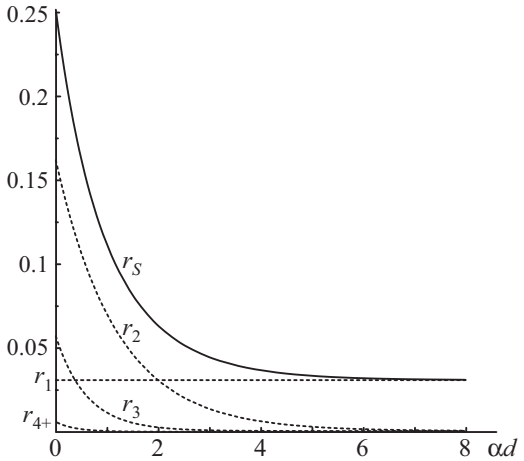

Fig. 3. Evolution of r_1, r_2, r_3, r_{4+}, and r_S as functions of diametrical absorbance.

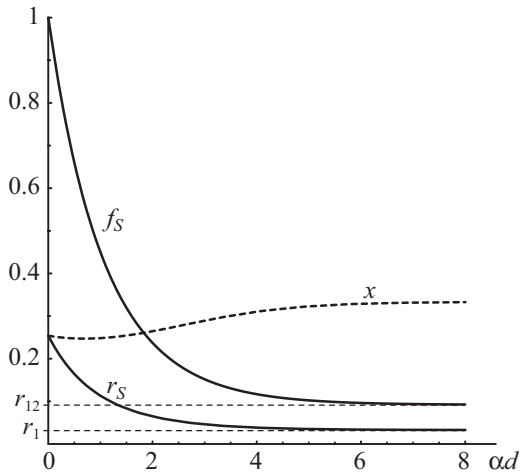

Fig. 4. Backward component r_S, diffuse nonabsorbance f_S and backscattering ratio $x=r_S/f_S$ as functions of diametrical absorbance.

It strongly depends on the binder-particle relative refractive index n_2/n_1 as shown in Fig. 5. A high relative refractive index increases Fresnel's reflectivities and therefore favors the backscattering.

6. PARTICLE SUBLAYER

As a first step for considering several particles within the particle medium, we select a thin sublayer containing almost coplanar particles called the particle sublayer. The binder is a perfectly clear medium 1, and the particles are identical, large, spherical, and made of an absorbing and nonscattering medium 2, such as in Sections 3–5. We would like to express the reflectance and the transmittance of the particle sublayer. Since there is some space between the particles, only a fraction a, called the shadowing ratio, of the diffuse incoming light interacts with the particles. This part of light is backscattered within a proportion of r_S, i.e., the backward component presented in Section 5. Therefore, the reflectance r_L of the particle sublayer is

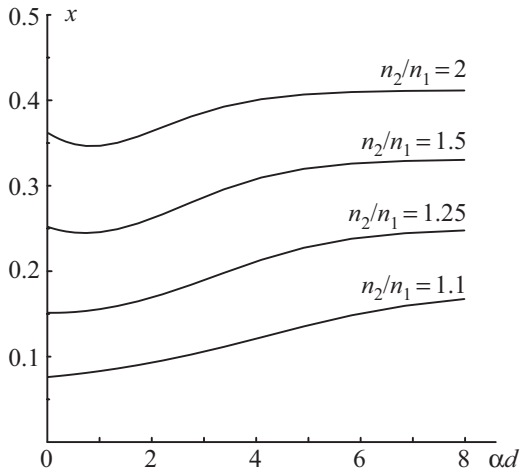

Fig. 5. Evolution of the backscattering ratio as functions of diametrical absorbance for various relative refractive indices.

$$r_L = a\ r_S = axf_S, \tag{50}$$

where x is the backscattering ratio defined in Eq. (33). The particle sublayer transmittance is formed by the fraction $(1-a)$ of incident light that does not strike any particle and by the fraction a of light scattered forward by the stroked particles

$$t_L = 1 - a + a(1-x)f_S. \tag{51}$$

The multiple reflections of light between neighboring particles (lateral scattering) and the shadowing of each particle by its neighboring particles are ignored, assuming that the overestimation of incident light due to omission of shadowing is compensated by the underestimated attenuation of scattered light due to lateral scattering.

We may extend the model by considering a colored binder with absorption coefficient α_M instead of a clear binder. In this case, the particle layer is a slice of binder whose thickness equals the diameter d of the particles. A light ray perpendicularly crossing the slice is attenuated by a factor $t=e^{-\alpha_M d}$ given by Beer's law [Eq. (2)]. An oblique ray crossing it according to an angle θ is attenuated by the factor $t^{1/\cos\theta}$. Diffuse light is attenuated by a factor t_M that embodies the attenuation of all the ray orientations

$$t_M = \int_{\theta=0}^{\pi/2} e^{-\alpha_M d/\cos\theta} \sin 2\theta \mathrm{d}\theta. \tag{52}$$

In a first approximation, we may consider that the binder significantly attenuates only the fraction (1–a) of incident light that does not strike any particle. The rest of the incident light, which interacts with the particles, travels almost no distance within the binder and can be assumed as not absorbed outside the particle. Thus, Eq. (50) is unchanged and Eq. (51) becomes

$$t_L = (1-a)t_M + a(1-x)f_S. \tag{53}$$

The particle sublayer can also be composed of various types of particles with different refractive indices, diameters, and/or absorption coefficients. Each type of particle is characterized by its nonabsorbance f_Sk, its backscattering ratio x_k, and its shadowing ratio a_k, where the sum of the a_k is lower than 1. Equations (50) and (51) become, respectively,

$$r_L = \sum_{k=1}^{N} a_k x_k f_{Sk} \tag{54}$$

and

$$t_L = 1 - \sum_{k=1}^{N} a_k + \sum_{k=1}^{N} a_k(1-x_k)f_{Sk}. \tag{55}$$

7. INFINITE PARTICLE MEDIUM

According to our model, an infinitely thick particle medium corresponds to a semi-infinite pile of particle sublayers. This section aims at determining its reflectance and examining its evolutions as a function of absorption, refractive index, and shadowing ratio.

A. Infinite Reflectance

Let us consider a semi-infinite pile of particle sublayers with Lambertian light illuminating the first layer. The first layer has a reflectance r_L, given by Eq. (50), and a transmittance t_L, given by Eq. (51). The second layer together with all lower layers form a reflecting background whose directional reflectance is r_∞. Figure 6 shows the multiple reflection process taking place between the first layer and this reflecting background. Summing the exiting components featured in Fig. 6 yields a geometric series, such as the model of Kubelka [13]. After reduction, the reflectance $r_{1+\infty}$ of the infinite particle medium is

$$r_{1+\infty} = r_L + \frac{t_L^2 r_\infty}{1 - r_L r_\infty}. \tag{56}$$

Since the number of particle sublayers is infinite, reflectance $r_{1+\infty}$ is not influenced by the addition or the subtraction of one layer, i.e., $r_{1+\infty} \equiv r_\infty$. Equation (56) yields the following equation:

$$r_\infty^2 - \frac{1 + r_L^2 - t_L^2}{r_L} r_\infty + 1 = 0 \tag{57}$$

whose single valid solution (the other solution is higher than 1 and cannot represent a reflectance) is

$$r_\infty = \frac{1 + r_L^2 - t_L^2}{2r_L} - \sqrt{\left(\frac{1 + r_L^2 - t_L^2}{2r_L}\right)^2 - 1}. \tag{58}$$

According to Eq. (58), we may express reflectance r_∞ under the form

$$r_\infty = A - \sqrt{A^2 - 1} \tag{59}$$

and replace r_L and t_L according to Eqs. (50) and (51), which yields

$$A = \frac{(1 - f_S)}{2x f_S} + (1 - a(1 - f_S))\left(1 + \frac{(1 - f_S)}{2x f_S}\right). \tag{60}$$

Since in the case of clear particles there is no absorption, we have $\alpha = 0$, $f_S = 1$, and thereby $r_\infty = 1$ independently of the shadowing ratio a and the refractive index n_2/n_1. Therefore, an infinite nonabsorbing particle medium reflects all of the light that it receives.

B. Numerical Evaluations

Figure 7 shows that the reflectance r_∞ of the infinite particle medium decreases as the particle absorbance αd increases for every binder-particle relative refractive index

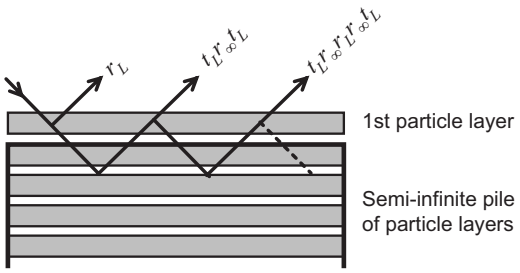

Fig. 6. Infinitely thick particle medium modeled as an infinite number of particle sublayers.

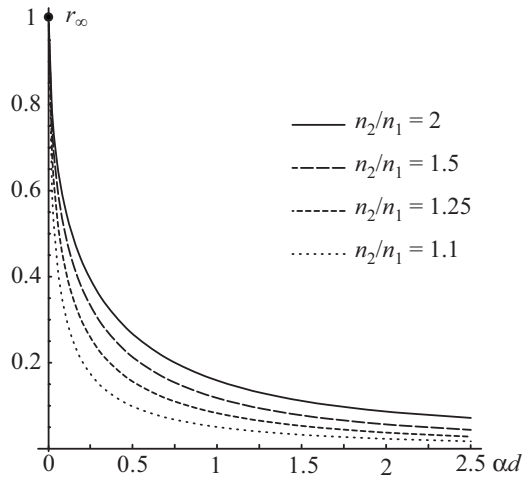

Fig. 7. Infinite particle medium reflectance as a function of diametrical absorbance for various relative refractive indices with a shadowing ratio $a = 0.5$.

n_2/n_1. Above a certain particle absorbance, since almost all of the light penetrating the particles is absorbed, only the light reflected on the external face of the particles is able to emerge from the particle medium, and the reflectance r_∞ becomes independent of the particle absorbance. A high binder-particle relative refractive index n_2/n_1 increases the reflectance r_∞ whatever the particle absorbance. The high Fresnel reflectivities favor the external reflections on the particles, and the low Fresnel transmittivities reduce the penetration and the absorption of light into particles.

The influence of the shadowing ratio is illustrated in Fig. 8, where r_∞ is plotted as a function of the diametrical absorbance αd for a small shadowing ratio $a = 0.005$ (dashed curve) or for a high shadowing ratio $a = 1$ (solid curve). The increase of reflectance r_∞ with the shadowing ratio, being up to 45% for a high particle absorbance, is consistent with the fact that interparticle multiple scattering is favored by closer particles.

8. INFINITE PARTICLE MEDIUM OBSERVED FROM AIR

In many cases, the binder refractive index n_1 is different from the refractive index of air, where the observer is lo-

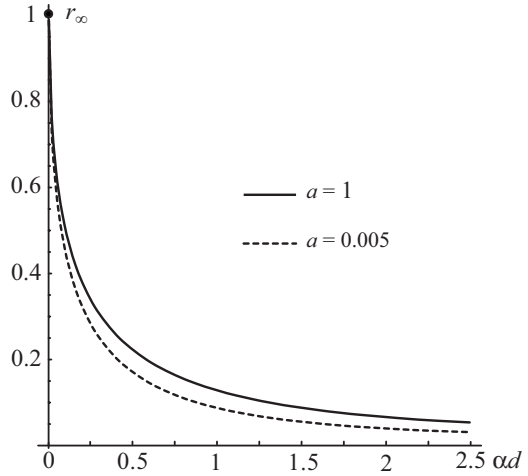

Fig. 8. Evolution of the infinite particle medium reflectance as a function of diametrical absorbance for various shadowing ratios.

cated. The reflections and transmissions of light at the binder–air interface must be taken into account. The particle medium, composed of a perfectly clear binder (medium 1) with particles made from a transparent medium 2, is assumed to have an infinite thickness and to behave as a Lambertian reflector with reflectance r_∞ given by Eq. (58). Its interface with air is assumed to be flat (Fig. 9). Due to the multiple reflections of light taking place beneath the air–binder interface and to the cone spreading of the observer's viewing solid angle at the interface, the global reflectance of the particle medium observed from air is not r_∞. Instead, the specimen is characterized by a reflectance factor ρ, which depends on the illumination and the observational geometries.

Directional incident light comes from the exterior at angle θ_0. A fraction $T_{01}(\theta_0)$, given by Fresnel's formulas, crosses the binder-air interface and is subject to multiple reflections between the stack of particles and the interior face of the upper interface. Since the light reflected back by the particles is Lambertian, the internal face of the flat interface has the internal diffuse reflectance r_{10} defined by Eq. (12), which depends on the refractive indices n_0 and n_1. The light emerging into the external medium is captured by a radiance detector at an angle θ_0'. The radiance captured by the detector at angle θ_0' is a fraction $(n_0/n_1)^2 T_{01}(\theta_0')$ of the radiance emitted by the particles itself being a fraction $1/\pi$ of the Lambertian irradiance reflected by the infinite stack of particles [31].

The global reflectance of the specimen, divided by the radiance to irradiance ratio $1/\pi$ of a perfect white diffuser, gives the global reflectance factor $\rho(\theta_0,\theta_0')$ of the specimen illuminated at angle θ_0 and observed at angle θ_0'

$$\rho(\theta_0,\theta_0') = (n_0/n_1)^2 T_{01}(\theta_0) T_{01}(\theta_0') \frac{r_\infty}{1 - r_\infty r_{10}}. \qquad (61)$$

The same expression would be obtained by applying Saunderson's correction [32] to the reflectance r_∞ of the stack of particles by considering a bidirectional measuring geometry. We assume that $\theta_0' \neq \theta_0$ so that gloss is discarded from the observation. Instead of directional incident light, we may have a diffuse light. The illumination is assumed to be Lambertian when the incident light coming from all directions of the upper hemisphere have the same radiance. This assumption only changes the Fresnel transmission of the incident light across the air–binder interface, which becomes t_{01} as defined by Eq. (13). When diffuse illumination is used, the radiance detector is usually positioned at the normal of the specimen, i.e., $\theta_0' = 0$ (diffuse/0° geometry). The reflectance factor $\rho(d,0)$ measured according to the diffuse/0° geometry is

$$\rho(d,0) = (n_0/n_1)^2 t_{01} T_{01}(0) \frac{r_\infty}{1 - r_\infty r_{10}}. \qquad (62)$$

Note that, according to Eq. (15), we have $t_{01} = (1 - r_{10})/(n_0/n_1)^2$. The reflectance factor becomes

$$\rho(d,0) = (1 - r_{10}) T_{01}(0) \frac{r_\infty}{1 - r_\infty r_{10}}.$$

Figure 10 shows the evolution of the reflectance factor $\rho(d,0)$ as a function of the diametrical absorbance, for the typical particle refractive index of chalk, $n_2 = 1.65$. The refractive index of the binder is $n_1 = 1$ for air, $n_1 = 1.33$ for water or $n_1 = 1.5$ for oil, and the refractive index of the external medium is $n_0 = 1$ (air). Like the infinite reflectance r_∞, the reflectance factor $\rho(d,0)$ decreases as the particle absorbance increases. The reduction of reflectance due to a high value of n_1 is first explained by the low value of the binder-particle refractive index n_2/n_1, which reduces the reflectance r_∞ (see Fig. 7), and second by the high value of the binder-air relative refractive index n_1/n_0, which increases the internal reflection of light beneath the air-binder interface and the chance for the light to be absorbed into particles.

In a dry powder, pigments are surrounded by air (binder refractive index close to 1). An important fraction of light emerges from the medium after reflections at the exterior of the pigments without absorption. This fraction of light has a constant spectrum and a white color. At the same time, the proportion of light penetrating the particles is low. This explains the bright and weakly saturated color of dried pigment powders. When the powder is mixed with oil (binder refractive index close to 1.5), less light is externally reflected on the pigments, and more light is absorbed inside them. This yields a strong contrast between spectral domains of high and of low absorbance and therefore a more saturated color for the pigment powder in oil.

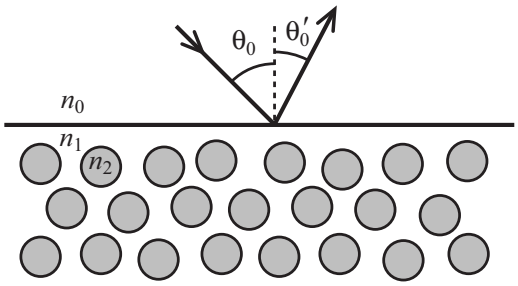

Fig. 9. Spherical transparent particles in a clear binding medium forming a flat interface with a different external medium.

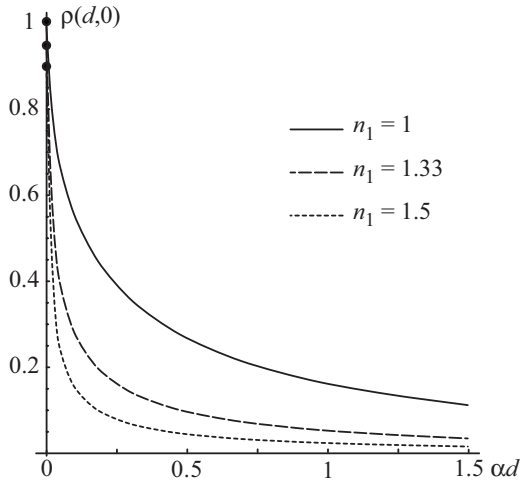

Fig. 10. Infinite particle medium reflectance factor as a function of the diametrical absorbance for various binder refractive indices $n_1 (n_2 = 1.65)$ and for a diffuse/0° measuring geometry in air.

In the special case, where the binder has the same refractive index as the particles ($n_2=n_1$), saturation would be optimal, but since the particle medium is infinite and there are no more reflections, the reflectance factor of the particle medium is zero, i.e., its color is black.

9. COMPARISON WITH THE MODEL OF SHKURATOV *et al.*

Except for the derivation of a reflectance factor, accounting for the multiple reflections of light beneath the air-binder interface, the model we propose relies on the same notions as the classical reflectance models for infinite particle media: Nonabsorbance of a single particle, backward component, reflectance and transmittance of a particle sublayer, and multiple reflections and transmissions among superposed particle sublayers. We propose to compare our model with the model of Shkuratov *et al.*, which is the closest to the model we have presented. The main differences concern the particle nonabsorbance and the derivation of the backward component.

A. Nonabsorbance

In the particle nonabsorbance model developed by Shkuratov *et al.* [22], the events of reflection and transmission are described for diffuse light. They are each represented by an average reflection or transmission factor. The light coming from the exterior of the particle is assumed to be Lambertian. A fraction r_{12} defined by Eq. (12) is reflected at the particle exterior surface, and a fraction t_{12} given by Eq. (13) is transmitted into the particle. The light located within the particle is also assumed to be Lambertian. A fraction r_{21} is reflected on the particle interior surface, and a fraction t_{21} is transmitted to the exterior. Attenuation due to absorption is also represented by an averaged factor M derived from Beer's law

$$M = e^{-\alpha \bar{d}}, \tag{63}$$

where $\bar{d}$ represents the average distance traveled by the light rays within the particle. It is calculated as the mean of the path lengths $d\cos\theta_2$ traveled by the light rays according to their orientation θ_2, knowing that rays oriented by angle θ_2 form a fraction $\sin 2\theta_2 d\theta_2$ of the global light flux

$$\bar{d} = \int_{\theta_2=0}^{\pi/2} d\cos\theta_2 \sin 2\theta_2 \mathrm{d}\theta_2 = \frac{2d}{3}. \tag{64}$$

The Lambertian light is subject to a multiple reflection-transmission process within the particle. Its description is similar to the description performed in Subsection 4.A for directional light and leads to a formula similar to Eq. (27) containing a geometric series

$$f_S = r_{12} + t_{12}t_{21}M\sum_{k=0}^{\infty}[r_{21}M]^k = r_{12} + \frac{t_{12}t_{21}M}{1-r_{21}M}. \tag{65}$$

Equation (65) was also derived by Melamed [19] under the same assumptions but with a different definition for the factor M. It is a sum of attenuated flux elements, each flux element corresponding to a fraction $\sin 2\theta_2 \mathrm{d}\theta_2$ of the initial flux with θ_2 as its orientation angle and being attenuated by the factor $\exp(-\alpha d\cos\theta_2)$ according to Beer's law [Eq. (26)]

$$M = \int_{\theta_2=0}^{\pi/2} e^{-\alpha d\cos\theta_2}\sin 2\theta_2 \mathrm{d}\theta_2 = \frac{2}{(\alpha d)^2}(1-(\alpha d+1)e^{-\alpha d}). \tag{66}$$

Figure 11 compares the diffuse nonabsorbance given by our model [Eq. (31)], by the model of Shkuratov *et al.* [Eq. (65) with M given by Eq. (63)], and by Melamed's model [Eq. (65) with M given by Eq. (66)]. Nonabsorbance is plotted as a function of the particle's diametrical absorbance αd for a relative refractive index $n_2/n_1=1.5$. The three curves are similar and with the same order of magnitude. However, the relative difference between our model and the models of Melamed or Shkuratov *et al.* reaches 20% due to the assumptions of Melamed and Shkuratov *et al.* of Lambertian light inside the particle. In the case of perfectly smooth spherical particles, light inside the particle is not Lambertian because it is refracted from the exterior medium to the particle medium of higher refractive index within a limited cone (and not within an entire hemisphere). In Appendix A, we propose an extension of the models of Melamed and Shkuratov *et al.* accounting for this limited cone in the special case of perfectly smooth spherical particles.

B. Backward Component

Shkuratov *et al.* proposed a model for quantifying backscattering and determining the backward component reflected by a particle. The model of Shkuratov *et al.* and our model differ in the definition of "backward" and "forward" directions for scattering. According to our model, the backward component only comprises light rays scattered into the hemisphere of incidence of the diffuse light (the upper hemisphere). In the model of Shkuratov *et al.*, the backward hemisphere is different for each incident ray. It is the hemisphere whose base is orthogonal to

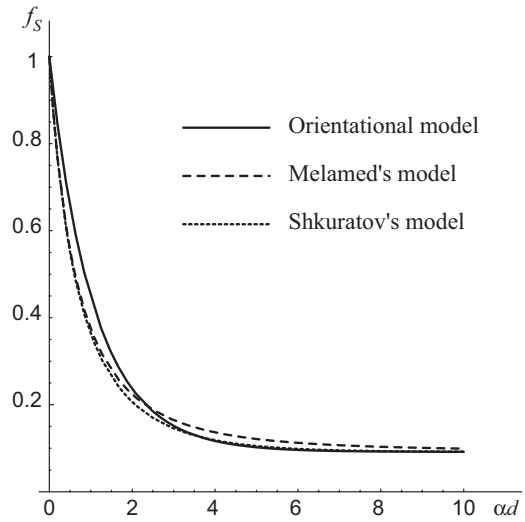

Fig. 11. Diffuse nonabsorbance f_S given by our model (solid curve), Melamed's model (dashed curve), and the model of Shkuratov *et al.* (dotted curve) as functions of the diametrical absorbance.

the incident ray. Thus, the backscattered rays are those that form an acute angle with the incident ray.

Let us consider the case of the first scattered rays reflected on the exterior surface of the particle. According to Snell's law, their angle with respect to their incident ray is twice the local incident angle. Therefore, according to the model of Shkuratov *et al.*, they are considered to be backscattered when the local incident angle is inferior to $\pi/4$. Their contribution r_1 to the backward component is

$$r_1 = \int_{\theta_1=0}^{\pi/4} R_{12}(\theta_1)\sin 2\theta_1 \mathrm{d}\theta_1. \tag{67}$$

Since the second scattered rays undergo two refractions when crossing the particle, their exiting direction depends on the relative refractive index of the binder-particle interface. Shkuratov *et al.* observed that for a relative refractive index inferior or equal to 1.5, almost all of the exiting rays form an obtuse angle with their incident ray. Assuming that this observation is also valid for higher relative refractive indices, the model of Shkuratov *et al.* neglects their contribution to the backward component. The third and following scattered rays are assumed to equally contribute to the backward and the forward components.

In Fig. 12, the backward component r_S calculated according to the model of Shkuratov *et al.* (dashed curve) and the one calculated according to our model (solid curve) are plotted as functions of the particle absorbance. The two horizontal lines represent the components r_1 derived according to the two models [Eqs. (49) and (67), respectively]. They represent the contribution of the first scattered rays that is independent of the particle absorbance. The contribution of the other scattered rays, dependent on the particle absorbance, is represented by a term r_a. According to Shkuratov *et al.*, r_a is half the total scattered flux composed of the third and following scattered rays. According to our model, r_a gathers the terms r_2, r_3, and r_{4+} plotted in Fig. 3. The differences in the definitions of the backward and forward directions induce significant differences between the terms r_S, r_1, and r_a derived according to our model and according to the model of Shkuratov *et al.* model.

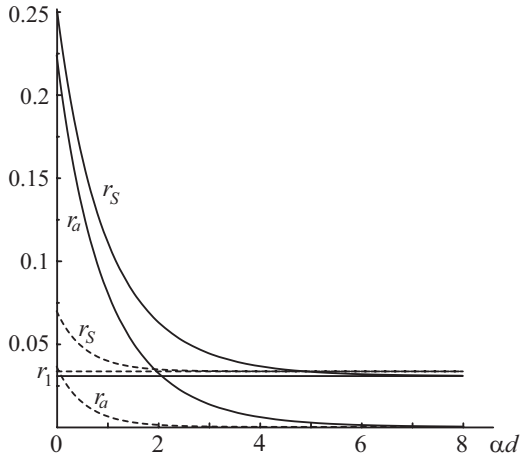

Fig. 12. Backward component r_s and contribution r_a of the second and following scattered rays according to our model (solid curve) and to the model of Shkuratov *et al.* (dashed curve) as functions of the particle absorbance.

In the multiple scattering model used by Shkuratov *et al.* and by us, the backward component represents the contribution of a single particle to the particle sublayer reflectance. In contrast to the approach by Shkuratov *et al.*, our computation of the backward component only comprising the light rays scattered in the hemisphere of incidence of the diffuse light is consistent with Kubelka's layering model [13] applied for computing the reflectance of a pile of particle sublayers (e.g., Subsection 7.A).

10. CONCLUSIONS

The proposed reflectance model is dedicated to particle media formed by a collection of large, identical, absorbing, and spherical particles contained within a clear binder. Five parameters are used: The refractive index of the particles, their size, their absorption coefficient, their concentration represented by the shadowing ratio, and the refractive index of the binder. The model relies on the notion of the particle sublayer whose reflectance and transmittance are obtained by describing the multiple reflection-transmission of light inside a single particle. The backscattering of a particle is calculated by considering the attenuation and the direction of each scattered light ray according to a 3D-vector model, assuming a Lambertian illumination from the upper hemisphere. The infinite particle medium corresponds to an infinite pile of particle sublayers. Its reflectance is obtained by describing the multiple reflection-transmission of diffuse light between the particle sublayers. The model is extended to the case of a binder different from air, where both the internal light reflections beneath the binder-air interface and the measuring geometry have an importance. The differences between our model and the recent model of Shkuratov *et al.* are also examined. The influences of the particle absorption coefficient, the particle shadowing ratio, and the particle and binder refractive indices on the reflectance of an infinite particle medium are illustrated by numerical evaluations. The present model enables one to predict the reflection spectrum of a particle medium and therefore estimate the variation of its color, brightness, or saturation when the particle concentration or the binder refractive index are modified. It provides a helpful framework for predicting the aspect of powders and may be used for the color formulation of pigmented paints.

APPENDIX A

The models of Shkuratov *et al.* and of Melamed for the multiple reflection and transmission of diffuse light within a particle are presented in Subsection 9.A. Their expression for the diffuse nonabsorbance of a spherical transparent particle notably differs from the one given by our model. This is because, in the case of transparent particles whose refractive index is higher than the refractive index of the surrounding medium ($n_2 > n_1$), the orientation of light rays refracted into the particle cannot exceed the critical angle $\theta_L = \arcsin(n_1/n_2)$. Since, for each light ray, the multiple reflection process occurs with an identi-

cal incidence angle for each reflection, and since there is no diffusion, it is impossible to have Lambertian light, i.e., rays of equal radiance propagating over the whole hemisphere inside the particle.

Assuming that the diffuse light is uniformly distributed over the angular range $[0, \theta_L]$, the average attenuation factors should be expressed by integrals between 0 and θ_L instead of the integrals between 0 and $\pi/2$ expressing r_{21} in Eq. (12) or M in Eq. (66). The diffuse internal reflectance $\tilde{r}_{21}$ of the particle interface becomes

$$\tilde{r}_{21} = \frac{\int_{\theta_2=0}^{\arcsin(n_0/n_1)} R_{21}(\theta_2)\sin 2\theta_2 \mathrm{d}\theta_2}{\int_{\theta_2=0}^{\arcsin(n_1/n_2)} \sin 2\theta_2 \mathrm{d}\theta_2} = \frac{(n_1/n_2)^2 r_{12}}{(n_1/n_2)^2} = r_{12} \tag{A1}$$

with the integrals being reduced due to the change of variable $\theta_2 = \arcsin(n_1/n_2 \sin\theta_1)$ and the identity $R_{21}(\theta_2) = R_{12}(\theta_1)$. We observe that the spherical interface has the same diffuse reflectance at the interior and exterior. Thus, the diffuse nonabsorbance given by Eq. (65) becomes

$$f_S = r_{12} + \frac{(1-r_{12})^2 M}{1 - r_{12} M}. \tag{A2}$$

Regarding the average attenuation factor M due to absorption, the average travel length used in the model of Shkuratov *et al.* Eq. (64) becomes

$$\bar{d} = \frac{\int_{\theta=0}^{\arcsin(n_1/n_2)} d\cos\theta \sin 2\theta \mathrm{d}\theta}{\int_{\theta=0}^{\arcsin(n_1/n_2)} \sin 2\theta \mathrm{d}\theta}, \tag{A3}$$

and the factor M then becomes

$$M = \exp(-\alpha\bar{d}) = \exp[-(2/3)\alpha d (n_2/n_1)^2 (1-\mu^3)] \tag{A4}$$

with

$$\mu = \sqrt{1-(n_2/n_1)^2}. \tag{A5}$$

According to Melamed's model, the average attenuation factor becomes

$$M = \frac{\int_{\theta=0}^{\arcsin(n_1/n_2)} e^{-\alpha d\cos\theta} \sin 2\theta \mathrm{d}\theta}{\int_{\theta=0}^{\arcsin(n_1/n_2)} \sin 2\theta \mathrm{d}\theta}, \tag{A6}$$

i.e., with μ given by Eq. (A5)

$$M = \frac{2(n_2/n_1)^2}{(\alpha d)^2}[e^{-\alpha d\mu}(1+\alpha d\mu) - e^{-\alpha d}(1+\alpha d)]. \tag{A7}$$

The improved models of both Shkuratov *et al.* and Melamed give nearly the same diffuse nonabsorbance as our model with relative differences lower than 1% for a relative refractive index $n_2/n_1 = 1.5$.

REFERENCES

1. C. F. Bohren and D. R. Huffman, *Absorption and Scattering of Light by Small Particles* (Wiley-Interscience, 1983).
2. M. Born and E. Wolf, *Principles of Optics*, 7th ed. (Pergamon, 1999).
3. H. C. van de Hulst, *Light Scattering by Small Particles* (Dover, 1981), pp. 200–227.
4. S. Chandrasekhar, *Radiative Transfer* (Dover, 1960).
5. K. Stamnes, S. Chee Tsay, W. Wiscombe, and K. Jayaweera, "Numerically stable algorithm for discrete-ordinate-method radiative transfer in multiple scattering and emitting layer media," Appl. Opt. **27**, 2502–2510 (1988).
6. L. Simonot, M. Elias, and E. Charron, "Special visual effect of art glazes explained by the radiative transfer equation," Appl. Opt. **43**, 2580–2587 (2004).
7. P. S. Mudgett and L. W. Richards, "Multiple scattering calculations for technology," Appl. Opt. **10**, 1485–1502 (1971).
8. W. E. Vargas and G. A. Niklasson, "Applicability conditions of the Kubelka–Munk theory," Appl. Opt. **36**, 5580–5586 (1997).
9. P. Kubelka and F. Munk, "Ein Beitrag zur Optik der Farbanstriche," Z. Tech. Phys. (Leipzig) **12**, 593–601 (1931) (in German).
10. P. Kubelka, "New contributions to the optics of intensely light-scattering material, part I," J. Opt. Soc. Am. **38**, 448–457 (1948).
11. M. Hébert and R. D. Hersch, "Reflectance and transmittance model for recto-verso halftone prints," J. Opt. Soc. Am. A **23**, 2415–2432 (2006).
12. G. Stokes, "On the intensity of light reflected from or transmitted through a pile of plates," *Mathematical and Physical Papers of Sir George Stokes, IV* (Cambridge U. Press, 1904), pp. 145–156.
13. P. Kubelka, "New contributions to the optics of intensely light-scattering materials, part II: Non homogeneous layers," J. Opt. Soc. Am. **44**, 330–335 (1954).
14. G. Kortüm, *Reflectance Spectroscopy* (Springer-Verlag, 1969).
15. M. Vöge and K. Simon, "The Kubelka–Munk and Dyck paths," J. Stat. Mech.: Theory Exp. **2007**, P02018 (2007).
16. K. Simon and B. Trachsler, "A random walk approach for light scattering in material," Discrete Math. Theor. Comp. Sci. **AC**, 289–300 (2003).
17. M. Hébert, R. Hersch, and J.-M. Becker, "Compositional reflectance and transmittance model for multilayer specimens," J. Opt. Soc. Am. A **24**, 2628–2644 (2007).
18. Z. Bodo, "Some optical properties of luminescent powders," Acta Phys. Acad. Sci. Hung. **1**, 135–150 (1951).
19. N. T. Melamed, "Optical properties of powders: Part I. Optical absorption coefficients and the absolute value of the diffuse reflectance," J. Appl. Phys. **34**, 560–570 (1963).
20. A. Mandelis, F. Boroumand, and H. van den Bergh, "Quantitative diffuse reflectance spectroscopy of large powders: The Melamed model revisited," Appl. Opt. **29**, 2853–2860 (1990).
21. H. Garay, O. Eterradossi, and A. Benhassaine, "Should Melamed's spherical model of size-colour dependence in powders be adapted to non spheric particles?" Powder Technol. **156**, 8–18 (2005).
22. Y. G. Shkuratov, L. Starukhina, H. Hoffmann, and G. Arnold, "A model of spectral albedo of particulate surfaces: Implication to optical properties of the Moon," Icarus **137**, 235–246 (1999).
23. Y. G. Shkuratov and Y. S. Grynko, "Light scattering by media composed of semitransparent particles of different shapes in ray optics approximation: consequences for spectroscopy, photometry, and polarimetry of planetary regoliths," Icarus **173**, 16–28 (2005).
24. D. B. Judd, "Fresnel reflection of diffusely incident light," J. Res. Natl. Bur. Stand. **29**, 329–332 (1942).
25. M. Hébert and R. D. Hersch, "Classical print reflection models: A radiometric approach," J. Imaging Sci. Technol. **48**, 363–374 (2004).

26. *CRC Concise Encyclopedia of Mathematics* (CRC Press, 1998), p. 1580.
27. W. R. McCluney, *Introduction to Radiometry and Photometry* (Artech House, 1994).
28. C. F. Bohren and D. R. Huffman, *Absorption and Scattering of Light by Small Particles* (Wiley-Interscience, 1983), p. 172.
29. B. Mayer and S. Madronich, "Photolysis frequencies in water droplets: Mie calculations and geometrical optics limits," Atmos. Chem. Phys. Discuss. **4**, 4105–4130 (2004).
30. W. J. Glantschnig and S. H. Chen, "Light scattering from water droplets in the geometrical optics approximation," Appl. Opt. **20**, 2499–2509 (1981).
31. L. Simonot, M. Hébert, and R. Hersch, "Extension of the Williams–Clapper model to stacked nondiffusing colored coatings with different refractive indices," J. Opt. Soc. Am. A **23**, 1432–1441 (2006).
32. J. L. Saunderson, "Calculation of the color pigmented plastics," J. Opt. Soc. Am. **32**, 727–736 (1942).